Research Square

Preprints are preliminary reports that have not undergone peer review.
They should not be considered conclusive, used to inform clinical practice,
or referenced by the media as validated information.

# From K-snack to copolymer: Conversion of Silkworm pupa oil into poly(3- hydroxybutyrate-co-3-hydroxyhexanoate) by engineered Cupriavidus necator H16

**Geonwoo Doh**
Konkuk University
**Yuni Shin**
Konkuk University
**Tae Yun Kim**
Konkuk University
**Seung Hun Lee**
Konkuk University
**Yun-Gon Kim**
Soongsil University
**Hee Taek Kim**
Chungnam National University
**Woo-Young Jeon**
Korea Research Institute Bioscience Biotechnology (KRIBB)
**Jungoh Ahn**
Korea Research Institute Bioscience Biotechnology (KRIBB)
**Kwon-Young Choi**
Ajou University
**Shashi Kant Bhatia**
Konkuk University
**Yung-Hun Yang**
seokor@konkuk.ac.kr

Konkuk University

**Research Article**

**Keywords:** Silkworm pupa oil, Insect oil, P(3HB-co-3HHx), Polyhydroxyalkanoates, Cupriavidus necator, Biopolymer production

**Posted Date:** June 24th, 2026

**DOI:** https://doi.org/10.21203/rs.3.rs-9975695/v1

**License:** This work is licensed under a Creative Commons Attribution 4.0 International License.
Read Full License

**Additional Declarations:** No competing interests reported.

# From K-snack to copolymer: Conversion of Silkworm pupa oil into poly(3-hydroxybutyrate-*co*-3-hydroxyhexanoate) by engineered *Cupriavidus necator* H16

Geonwoo Doh[a], Yuni Shin [a], Tae Yun Kim [a], Seung Hun Lee [a], Yun-Gon Kim [b], Hee Taek Kim [c], Woo-Young Jeon[d], Jungoh Ahn[d], Kwon-Young Choi[e,f], Shashi Kant Bhatia[a,g], Yung-Hun Yang[a,g*]

[a] Department of Biological Engineering, College of Engineering, Konkuk University, Seoul, Republic of Korea, 120 Neungdong-ro, Gwanjin-gu, Seoul 05029, Republic of Korea.

[b]Department of Chemical Engineering, Soongsil University, Seoul, Republic of Korea

[c]Department of Food Science and Technology, Chungnam National University, Daejeon, Republic of Korea

[d]Biotechnology Process Engineering Center, Korea Research Institute Bioscience Biotechnology (KRIBB), Chungbuk, Republic of Korea

[e]Department of Molecular Science and Technology, Ajou University, Suwon, Gyeonggi-do, Republic of Korea

[f]Advanced College of Bio-Convergence Engineering, Ajou University, Suwon, Gyeonggi-do, Republic of Korea

[g] Institute for Ubiquitous Information Technology and Application, Konkuk University, Seoul, Republic of Korea, 120 Neungdong-ro, Gwanjin-gu, Seoul 05029, Republic of Korea.

***Corresponding author**

Prof. Yung-Hun Yang

Department of Biological Engineering, College of Engineering

Konkuk University, Seoul 05029, Republic of Korea

**E-mail address:** seokor@konkuk.ac.kr

**Phone number:** (+82) 10-9079-9846

## Abstract

Silkworm pupae are continuously generated as a major byproduct of the silk industry and have long been consumed as inexpensive, high-energy snacks in Korea. However, consumer acceptance has become increasingly variable due to their distinctive appearance and odor. Gas chromatography–mass spectrometry (GC–MS) analysis revealed that silkworm pupa oil (SPO) consists of approximately 54% oleic acid, 29% linoleic acid, 17% palmitic acid, and minor amounts of cyclopropane fatty acids. Based on this composition, this study evaluated the feasibility of producing poly(3-hydroxybutyrate-*co*-3-hydroxyhexanoate) [P(3HB-*co*-3HHx)] using engineered *Cupriavidus necator* H16 with SPO as a sustainable substrate. Compared with other carbon sources, SPO supported comparable growth and polyhydroxyalkanoate (PHA) content, which was 2.64-fold higher than fructose and 1.42-fold higher than bean oil in flask cultures, demonstrating its potential as an efficient substrate. Supplementation with 1.0% fructose as an auxiliary carbon source further increased dry cell weight (DCW) and total PHA accumulation by up to 20%. To improve emulsification, various emulsifiers were screened, and Tween 20 enhanced DCW and PHA yield by 1.4-fold and 1.55-fold, respectively. The resulting film exhibited a tensile strength of 6.0 ± 0.6 MPa and an elongation at break of 53.4 ± 4.6%, and showed approximately 90% degradation after 7 days by *Microbulbifer* sp. SOL66. Overall, this study demonstrates that SPO is a promising and sustainable carbon source for PHA production, highlighting the valorization of silk industry byproducts into high-value biopolymeric materials.



**Keywords:** Silkworm pupa oil, Insect oil, P(3HB-*co*-3HHx), Polyhydroxyalkanoates, *Cupriavidus necator*, Biopolymer production

## 1. Introduction

Silkworm pupae are a major byproduct of the sericulture industry, which is primarily dedicated to silk fiber production. After silk is reeled from cocoons, substantial amounts of pupae remain and have traditionally been regarded as low-value residues [1,2]. However, silkworm pupae are rich in proteins and lipids, making them a valuable resource for nutritional and industrial applications [2,3]. In Korea, they have long been consumed as food, commonly in the form of *beondegi-tang* or canned snacks, and represent a distinctive component of traditional dietary culture [1,4]. Recently, they have gained attention as sustainable sources of proteins and bioactive ingredients, with expanding applications in the food, feed, and cosmetic industries [1–3]. However, consumer acceptance is increasingly polarized due to their distinctive appearance and odor, particularly among younger generations. These limitations suggest that reliance on food-based utilization alone may not be sustainable [4,5]. Silkworm pupa oil (SPO) is a valuable material owing to its nutritional and functional properties [2,3,5]. Its fatty acid profile is characterized by high levels of unsaturated fatty acids, including oleic acid (C18:1) and linoleic acid (C18:2), along with saturated fatty acids such as palmitic acid (C16:0) (Table 2). As a result, SPO shares characteristics with conventional vegetable oils while retaining distinct nutritional and functional features.

Polyhydroxyalkanoates (PHAs) are biodegradable and biocompatible polyesters synthesized by various microorganisms, including *Cupriavidus necator*, *Halomonas* spp., and *Pseudomonas* spp. [6,7]. These polymers accumulate as intracellular granules under excess carbon and limited nutrients such as nitrogen or phosphorus [6,7]. Due to their biodegradability, biocompatibility, and potential to replace petroleum-based plastics, PHAs have attracted significant attention as sustainable alternatives [7,8]. Among them, poly(3-hydroxybutyrate) (PHB) is the most extensively studied and the most commonly synthesized homopolymer.

However, large-scale commercialization remains limited due to high production costs, particularly those associated with expensive carbon substrates and energy-intensive downstream processing, which reduce competitiveness with petrochemical plastics [7,8]. To address this limitation, considerable effort has focused on inexpensive and renewable feedstocks, including agricultural residues, industrial byproducts, and food waste, as alternative carbon sources [6–8].

In this context, SPO is an attractive yet underexplored feedstock for producing value-added biopolymers. As a lipid-rich sericulture byproduct, it offers advantages in both waste valorization and cost reduction. Oil-based substrates are particularly suitable for PHA biosynthesis because fatty acid-derived carbon sources can support polymers accumulation with broader monomer compositions and improved material properties compared with PHB alone [9–16]. Among PHA-producing microorganisms, *C. necator* is widely recognized as an efficient and robust production host due to its high PHA productivity and ability to utilize diverse carbon sources, including plant oils and other lipid-based substrates [6,7,14]. However, the feasibility of using SPO as a carbon source for PHA production remains insufficiently explored.

In this study, we evaluated SPO as a low-cost carbon source for PHA production by *C. necator*. To improve the availability of hydrophobic substrates in aqueous cultures, emulsification strategies were applied. The performance of SPO was compared with that of other oil-based substrates, and the resulting polymers were characterized in terms of physicochemical properties. This study demonstrates the feasibility of valorizing SPO for cost-effective PHA production and highlights its potential as a sustainable feedstock for the synthesis of value-added biopolymers, including P(3HB-*co*-3HHx).

## 2. Methods and materials

### *2.1. Strains and transformation*

The recombinant strain used was *Cupriavidus necator* H16 harboring pCB81. For routine cultivation, a pre-culture was prepared in 5 mL tryptic soy broth (TSB) and incubated for 24 h at 30 °C with gentamicin (50 μL/mL). Cells were harvested by 13,000rpm centrifugation, washed twice with sterile distilled water, and used as the inoculum. Unless otherwise stated, a 2% (v/v) seed culture was inoculated into *Ralstonia eutropha* minimal medium (ReMM). The medium was adjusted to pH 6.8 and contained 4 g/L $NaH_2PO_4$, 4.6 g/L $Na_2HPO_4$, 0.225 g/L $K_2SO_4$, 0.39 g/L $MgSO_4$, 62 mg/L $CaCl_2$, and 1 mL/L trace element solution. The trace element solution consisted of 15 g/L $FeSO_4 \cdot 7H_2O$, 2.4 g/L $MnSO_4 \cdot H_2O$, 2.4 g/L $ZnSO_4 \cdot 7H_2O$, and 0.48 g/L $CuSO_4 \cdot 5H_2O$ dissolved in 0.1 M HCl. Carbon and nitrogen sources varied depending on the experiment.

### *2.2. Fatty acid composition analysis by gas chromatography–mass spectrometry (GC–MS)*

SPO was diluted in chloroform to obtain a 1% (v/v) solution. Fatty acids were derivatized by mild alkaline methanolysis. Briefly, 0.5 mL methanol, 0.5 mL toluene, and 1 mL of 0.3 M methanolic KOH were added and incubated at 37 °C for 15 min. Then, 2 mL hexane, 0.3 mL 1 M acetic acid, and 2 mL of distilled water were supplemented, and the mixture was vortexed for phase separation. The upper hexane layer was collected, evaporated under nitrogen, resuspended in chloroform, dried over anhydrous $Na_2SO_4$, filtered through a 0.2 μm polyvinylidene fluoride (PVDF) membrane filter, and transferred to a vial. Analysis was performed using a Clarus 500 GC–MS system (PerkinElmer, Waltham, MA, USA) equipped with an Elite-5 ms capillary column (30 m × 0.25 mm i.d., 0.25 μm film thickness). The oven program was: 120 °C for 5 min, increased to 200 °C at 6 °C/min, increased to 220 °C at 2 °C/min,

and then increased to 300 °C at 10 °C/min. The injector temperature was set to 210 °C. Mass spectra were acquired using electron impact ionization at 70 eV over a scan range of 45–400 m/z.

### *2.3. Culture conditions*

To compare the substrate suitability for PHA production, *C. necator* H16 harboring pCB81 was cultivated in ReMM containing fructose, bean oil, or SPO as the carbon source. To examine the effect of SPO concentration, SPO was supplied at concentrations ranging from 0 to 3.0% (v/v) at 0.5% intervals. The nitrogen source in the medium was replaced with various inorganic or organic compounds concentration of 0.1% (w/v) to assess their effects, while SPO was supplied at the previously optimized condition of 1.5% (v/v). Time-dependent experiments were conducted using three carbon source conditions: 1% (w/v) fructose, 1.5% (v/v) SPO, and a combination of 1% fructose and 1.5% SPO. Samples were collected at designated time points to determine dry cell weight (DCW), PHA production, and PHA content. Agitation speed and cultivation temperature were varied to evaluate their effects on polymer production, as assessed by DCW, PHB production, and PHB content. Unless otherwise stated, media components were obtained from Sigma-Aldrich (St. Louis, MO, USA).

### *2.4. Fructose co-feeding optimization and residual fructose analysis*

For co-feeding optimization, *C. necator* H16 harboring pCB81 was cultivated in ReMM with 1.5% (v/v) SPO 0.1% urea, and fructose concentrations of 0, 0.5, 1.0, 1.5, 2.0, 2.5, and 3.0% (w/v). Cells were harvested and analyzed for DCW and PHA production. The effects of fructose concentration on biomass formation and polymer accumulation were compared to determine the optimal co-feeding conditions. For residual fructose analysis, culture broth was

centrifuged, washed once with distilled water and twice with hexane to remove residual oil, and the supernatants were filtered through a 0.22 μm PVDF membrane filter. Fructose concentration was measured by liquid chromatography equipped with a refractive index detector (LC-RID) with an Aminex HPX-87H column with 0.008 N $H_2SO_4$ as the mobile phase at 0.6 mL/min and 60 °C.

### *2.5. PHA analysis by gas chromatography–flame ionization detector (GC–FID)*

For DCW and PHA analysis, 1 mL culture medium was harvested after 72h cultivation, centrifuged, washed once with distilled water and twice with hexane to remove residual oil, and then lyophilized. DCW was determined gravimetrically based on the weight difference before and after lyophyilization. PHA was quantified by subjecting the lyophilized biomass to methanolysis using 1 mL chloroform and 1 mL 15% (v/v) $H_2SO_4$ in methanol at 100 °C for 2 h. Later then cooling, 1 mL of distilled water was added, and the organic phase was recovered. Residual water was removed with anhydrous $Na_2SO_4$, and the solution was filtered through a 0.22 μm PVDF membrane filter. Samples (1 μL) were analyzed using a gas chromatograph equipped with a flame ionization detector (GC–FID; YL6500, Young In Chromass, Korea) and an HP-FFAP capillary column (30 m × 0.32 mm i.d., 0.25 μm film thickness). Helium was used as the carrier gas at a flow rate of 3 mL/min. The injector temperature was set to 210 °C, the FID temperature was 230 °C, and the oven temperature was programmed from 80 to 220 °C. PHB and P(3HB-*co*-3HHx) were quantified using standard calibration curves [14,17].

### *2.6. Effect of emulsifier type and concentration on SPO utilization and PHA production*

To examine the effect of emulsification on the utilization of SPO during PHA production, Tween 20, Tween 80, Tween 85, and sodium dodecyl sulfate (SDS) were

individually added to ReMM at final concentrations of 0.05%, 0.10%, 0.15%, and 0.20% (w/v) with 1% fructose, 1.5% SPO, and 0.1% urea [18–21]. A culture without emulsifiers served as the control. Cultures were incubated at 37 °C for 72 h, after which DCW, PHA production, PHA content, and 3HHx mole fractions were measured. Effects were evaluated based on biomass, polymer accumulation, and copolymer composition. Light microscopy was used to compare oil droplet formation on the surface of the upper culture layer after 72h of cultivation in 100mL flask clutures, with or without emulsifier treatment.

### *2.7. Film preparation and physical characterization*

#### *2.7.1. Film production*

For film production, *C. necator* H16 harboring pCB81 was inoculated from a 100-mL flask culture into a 250-mL flask including ReMM-based medium with 1% fructose, 1.5% SPO, and 0.1% urea. After cultivation, the harvested cells were recovered by centrifugation and sequentially washed once with distilled water and twice with hexane to remove medium components and residual hydrophobic substrates. And then lyophilization was performed twice to ensure complete dryness. PHA was extracted by treating the dried biomass with 50 mL chloroform to the lyophilized cells for cell lysis, and extraction was performed at 60 °C for 2 h. Then filtered through Whatman No. 1 filter paper. The resulting PHA solution was poured into a glass Petri dish and allowed to dry at room temperature to form a film. For physicochemical characterization, 0.4 g of the prepared film was redissolved in 50 mL chloroform and recast using the same solvent evaporation method. The recast films were then subjected to gel permeation chromatography (GPC), universal testing machine (UTM), differential scanning calorimetry (DSC), water contact angle and thermogravimetric analysis (TGA) analyses [17,22].

196 *2.7.2. Gel permeation chromatography (GPC)*

197 Molecular weight analysis was performed using a GPC system (YL Chromass, Seoul,
198 Korea) equipped with a loop injector (Rheodyne 7725i), dual-head isocratic pump (YL9112),
199 column oven (YL9131), Shodex K-805 column (8.0 mm I.D. × 300 mm), and refractive index
200 detector (YL9170). Samples were prepared by dissolving 10 mg PHA film in 2 mL chloroform
201 and filtering through a 0.22 μm PVDF filter. A 20 μL air bubble-free sample was injected.
202 Chloroform was used as the eluent at a constant flow rate of 1 mL/min, and the column
203 temperature was kept at 40 °C. Molecular weight distributions were estimated relative to
204 polystyrene standards with molecular weights of 5,000–2,000,000 Da using YL-Clarity
205 software connected to the YL HPLC system[17,22].
206

207 *2.7.3. Universal testing machine (UTM)*

208 Mechanical characterization of H16-derived PHA films was performed using an EZ-
209 SX universal testing machine (UTM; Shimadzu, Kyoto, Japan). Rectangular film specimens
210 were prepared at a size of 60 × 20 mm², and specimen thickness was measured with a 1111–
211 100 A mini digital caliper (Insize, Loganville, GA, USA). Tensile tests were carried out at a
212 crosshead speed of 20 mm/min. The tensile strength, elongation at break, and Young's modulus
213 were calculated from the resulting stress–strain profiles using TRAPEZIUM X software [17,22].
214

215 *2.7.4. Differential scanning calorimetry (DSC)*

216 Thermal characterization of the H16-derived films was performed using a NEXTA
217 DSC 200 instrument (Hitachi, Tokyo, Japan). Glass transition temperature ($T_g$), crystallization
218 temperature ($T_c$), and melting temperature ($T_m$) were determined using 5.0-5.5 mg samples.

The analysis was conducted from −60 °C to 180 °C at heating and cooling rates of 10 °C/min under a nitrogen atmosphere, and mean values were obtained from repeated measurements [17].

*2.7.5. Water contact angle*

The surface hydrophobicity of the PHA films was evaluated by water contact angle measurement using a Phoenix-MT (M) contact angle analyzer (SEO, Suwon, Republic of Korea). Distilled water was employed as the probe liquid, and the contact angle was recorded after carefully placing a droplet onto the film surface with a syringe.

2.7.6. Thermogravimetric analysis (TGA)

TGA was performed using a TGA N-1000 instrument (Scinco, Korea). Thermal stability was evaluated over 40–550 °C under a high-purity nitrogen atmosphere. Gas flow rates were set to 20 mL/min at the upper inlet and 10 mL/min at the lower inlet.

*2.8. Time-dependent biodegradation of P(3HB-co-3HHx) films*

Time-dependent biodegradation was carried out using *Microbulbifer* sp. SOL66 in MB medium, with minor modifications to previously reported methods. This strain has been reported to exhibit high PHA-degrading activity, and its applicability for degrading P(3HB-*co*-3HHx) films has been demonstrated previously [23,24]. Film samples were prepared by dissolving 0.1g of the previously prepared polymer film in 50 mL of chloroform, followed by recasting into films. Aliquots corresponding to 20 mg film were added to MB medium and incubated for 3, 5, and 7 days. At each time point, films were recovered, washed to remove residual cells and medium components, and lyophilized. Recovered films were then subjected to methanolysis, followed by GC–FID analysis to determine residual polymer. The degradation

percentage was calculated based on the residual polymer amount relative to the initial film weight.

### *2.9. Statistical analysis*

All experiments were carried out in biological triplicates unless stated otherwise, and the results are reported as the mean ± standard deviation (SD). Statistical differences among groups were evaluated using one-way analysis of variance (ANOVA) followed by Tukey's post hoc multiple comparison test. A p-value of $< 0.05$ was considered statistically significant.

## 3. Results

### *3.1. Characterization of SPO and its suitability as a carbon source for PHA production*

GC–MS analysis was conducted to determine the major components of SPO and assess its suitability as a carbon source for PHA production. SPO was mainly composed of oleic acid (53.5%), linoleic acid (28.8%), and palmitic acid (16.8%), with a minor fraction of cyclopropane-containing fatty acids (Fig. 1A). This composition indicates that the oil contains a mixture of unsaturated and saturated fatty acids that can be effectively utilized for microbial PHA biosynthesis. Among the tested carbon sources, SPO supported the highest biomass formation and PHA production (Fig. 1B). Engineered *C. necator* H16 harboring pCB81, expressing enoyl-CoA hydratase (*phaJ*) from *Pseudomonas* sp., PHA synthase (*phaC*) from *Rhodococcus* sp., and β-ketothiolase (*phaA*), was used to produce poly(3-hydroxybutyrate-*co*-3-hydroxyhexanoate) [P(3HB-*co*-3HHx)], composed of 3-hydroxybutyrate (3HB) and 3-hydroxyhexanoate (3HHx) monomers [25]. Because *C. necator* H16 contains native *phaA,* acetoacetyl-CoA reductase (*phaB*), and *phaC*, fructose supports PHB production, whereas bean oil and SPO both enable the formation of a 3HHx-containing copolymer fraction of up to 9.6%

and 10.8%, respectively. Among these substrates, SPO yielded the highest DCW and P(3HB-*co*-10.3 mol% 3HHx), demonstrating its potential as an effective feedstock for oil-based PHA production.

### *3.2. Effect of SPO concentration and nitrogen source on PHB production*

To evaluate the effect of SPO concentration (0–3.0%, at 0.5% intervals) on polymer production was evaluated. Biomass formation and PHB production increased with SPO concentration up to 2.5%, indicating that increased carbon availability promoted both cell growth and polymer accumulation and increasing to 3.0% slightly reduced production. (Fig. 2A). However, the improvement at higher SPO concentraions was not sufficiently pronounced when all production parameters were considered collectively. Therefore, 1.5% SPO was selected as an appropriate concentration for subsequent experiments, providing a balanced condition for biomass formation and PHA accumulation. Nitrogen source also significantly affected PHB production (Fig. 2B). Urea provided the best performance, supporting the highest biomass and PHB production with high polymer content. In contrast, complex nitrogen sources (tryptone, yeast extract, and peptone) resulted in lower PHB titers despite moderate biomass formation. These results identify urea as the most suitable nitrogen source under the present cultivation conditions.

### *3.3. Evaluation of SPO as a substrate under different culture conditions*

As mixed-substrate feeding has been reported to improve biomass formation and polymer accumulation in *C. necator* grown on oil-based substrates, a time-dependent cultivation was performed to examine the effect of fructose supplementation on SPO-based PHA production (Fig. 3) [6,26]. Time-dependent cultivation experiments revealed distinct

291 growth and polymer accumulation patterns depending on the carbon source. Under fructose-
292 only conditions, cells exhibited rapid initial growth; however, final biomass and polymer
293 accumulation remained limited, and only PHB was detected (Fig. 3A). In contrast, cultures
294 supplied with 1.5% SPO showed higher biomass formation and production of both PHB and
295 3HHx, reaching up to 5.5 g/L and 0.8 g/L, respectively, indicating that SPO and fructose co-
296 feedeing supported copolymer biosynthesis (Fig. 3B). The co-feeding condition (1% fructose +
297 1.5% SPO) showed the most favorable performance, with PHA accumulation of 6.94 g/L, 3HHx
298 accumulation of 0.87 g/L, and a final PHA content of 51.7%, along with the highest biomass
299 (Fig. 3C). These findings are consistent with previous studies showing fructose supporting early
300 growth, whereas lipid substrates contributing more strongly to polymer accumulation and
301 copolymer formation [6,26]. Overall, fructose alone promoted early growth but limited final
302 polymer accumulation, whereas SPO enabled copolymer production and higher biomass. Their
303 combination integrates these advantages, improving both growth and polymer accumulation.
304
305 *3.4. Profile of fructose consumption and optimization of culture conditions*
306 To determine the effect of combinatorial carbon sources, fructose and SPO were used
307 together. In addition, further experiments were conducted to identify the culture conditions most
308 favorable for efficient polymer production. As fructose mainly supports the early growth phase,
309 whereas the lipid substrate contributes more to subsequent polymer accumulation and
310 copolymer formation, a positive synergy is expected. The fructose consumption profiles
311 differed between the fructose-only and co-feeding conditions (Fig. 4A,B). In the fructose-only
312 culture, residual fructose decreased rapidly and was depleted at approximately 30 h, after which
313 biomass formation plateaued with little further increase. Under co-feeding conditions, residual
314 fructose also declined during cultivation, indicating that fructose was primarily consumed

during the early growth phase. However, biomass continued to increase substantially even after fructose had decreased to a very low level, and this pattern was accompanied by greater polymer accumulation than that observed in the fructose-only culture. These observations suggest that fructose mainly supports early biomass formation, whereas SPO contributes to sustained growth and polymer accumulation during the later stages of cultivation. This complementary effect of fructose and oil co-feeding is consistent with previous reports on improved PHA production in *C. necator* under mixed carbon source conditions [6,26].

To optimize the co-feeding strategy, fructose concentration (0–3.0%, at 0.5% intervals) was varied while maintaining SPO at 1.5%. Increasing fructose concentration generally improved both biomass formation and PHB production, reaching up to 13.9 g/L and 6.07 g/L, respectively. Although 3.0% fructose yielded the highest values, the difference compared with 1.0% fructose was not substantial. Therefore, 1.0% fructose was selected as the optimal concentration for co-feeding. These results indicate that fructose supplementation improved polymer production in pupa-oil-fed cultures, with 1.0% fructose providing the most balanced overall performance within the tested range. Because oxygen supply and cultivation temperature are known to affect PHA accumulation in *C. necator*, agitation speed and temperature were further evaluated under the selected conditions (Fig. 5). Agitation had a clear effect on PHB production. As agitation speed increased from 0 to 300 rpm, both biomass formation and PHB accumulation increased markedly, indicating that mixing and oxygen transfer strongly influenced production efficiency. The highest biomass was obtained at 300 rpm, and PHB titers were also highest at higher agitation speeds. PHB content remained high at both 200 and 300 rpm, indicating that these conditions were more favorable than lower agitation settings. Overall, elevated agitation improved PHB production, with 200–300 rpm representing the most effective range under the tested conditions. Temperature also affected both growth and polymer accumulation. Biomass

formation and PHB production increased from 25 to 30 °C but decreased at temperatures above 30 °C. The lowest overall performance was observed at 37 °C. Although 28 °C and 33 °C still supported polymer production, neither exceeded the performance at 30 °C. These results indicate that 30 °C provided the most favorable balance between cell growth and PHB production under the present conditions.

### *3.5. Effect of emulsification on oil dispersion, PHA production, and copolymer composition*

Because SPO is a hydrophobic substrate, it was mainly present as floating droplets in the upper layer of the culture medium and was not readily dispersed under normal shaking conditions, which likely limited its accessibility to microbial cells. Previous studies on oil-based PHA production in *C. necator* have shown that the accessibility of lipid substrates can markedly influence polymer production efficiency [6,14]. To examine this effect, three non-ionic surfactants (Tween 20, Tween 80, and Tween 85) and the anionic surfactant SDS were evaluated under the same cultivation conditions (Fig. 6A and Table 2). The production data showed clear differences among the tested emulsifiers. SDS exhibited a strong inhibitory effect and almost completely suppressed both cell growth and PHA production at all tested concentrations. In contrast, Tween 20, Tween 80, and Tween 85 supported biomass formation and copolymer production. Among them, Tween 20 showed the most favorable performance, particularly at 0.10–0.15%, where the highest PHA content and one of the highest levels of biomass formation and PHB production were observed. Tween 80 and Tween 85 also supported copolymer formation, although their effects were generally lower or more variable than those of Tween 20. The 3HHx-containing copolymer fraction was consistently detected under Tween-supplemented conditions, and the 3HHx mole fraction remained within a comparable range across treatments. Taken together, these results indicate that appropriate emulsification

improves SPO utilization and promotes both PHA production and copolymer formation, whereas SDS was unsuitable under the tested conditions. Therefore, 0.1% Tween 20 was considered the most effective emulsifier condition.

Microscopic observations supported these trends (Fig. 6B,C). In the presence of emulsifiers, the oil phase was distributed as smaller and more uniformly dispersed droplets, whereas cultures without emulsifiers showed visible phase separation and larger droplets. These observations indicate that emulsification improves the physical availability of SPO in the aqueous medium, consistent with the improved production observed under Tween-based conditions. Similar relationships between oil utilization and substrate accessibility have been reported in previous studies on oil-fed *C. necator* cultures [14].

### *3.6. Production of P(3HB-co-3HHx) from SPO under optimized conditions*

Under optimized cultivation conditions, time-dependent experiments demonstrated sustained biomass formation and copolymer production throughout cultivation (Fig. 7). Both PHB and 3HHx fractions accumulated progressively, and PHA content increased markedly during later stages. The 3HHx mole fraction remained detectable over time, indicating stable biosynthesis of P(3HB-*co*-3HHx) rather than simple PHB accumulation. After 72h a DCW of 17.3 g/L was obtained, along with 11.84 g/L of 3HB and 1.63 g/L of 3HHx, corresponding to a PHA content of 70.2% and a 3HHx mole fraction of 11.25%. Collectively, these results indicate that SPO supports efficient copolymer production under the optimized conditions.

### *3.7. Film properties and biodegradation of SPO-derived P(3HB-co-3HHx)*

The solvent-cast film prepared from the SPO-derived polymer showed a number-average molecular weight ($M_n$) of 9.3 ± 0.3 × $10^5$, a weight-average molecular weight ($M_w$) of

$1.30 \pm 0.04 \times 10^6$, and a polydispersity index (PDI) of 1.4 ± 0.01 (Table 3). The film showed a water contact angle of 81.4 ± 0.2°, indicating a relatively hydrophobic surface. Mechanical testing yielded a tensile strength of 6.0 ± 0.6 MPa, elongation at break of 53.4 ± 4.6%, and Young's modulus of 127.09 ± 21.3 MPa. Thermal analysis showed a glass transition temperature ($T_g$) of -4.2 ± 1.7 °C, melting temperature ($T_m$) of 163.9 ± 2.4 °C, and crystallization temperature ($T_c$) of 107.7 ± 2.6 °C, while thermogravimetric analysis showed a maximum degradation temperature ($T_{max}$) of 283.6 °C and a residual mass of 8.3%. These results indicate that the SPO-derived polymer can be processed into films with defined molecular, thermal, and mechanical properties. This interpretation is consistent with previous studies showing that oil-fermented P(3HB-*co*-3HHx) exhibits measurable physicochemical properties and that the 3HHx fraction contributes to thermal and mechanical behavior [17,22]. Compared with previously reported P(3HB-*co*-3HHx) films, in which increasing 3HHx content generally decreases tensile strength and Young's modulus while improving flexibility, the SPO-derived film exhibited a low-modulus character, suggesting that the incorporated 3HHx fraction contributed to chain mobility rather than high tensile resistance [25,27,28]. In addition, the observed $T_g$ and $T_m$ values were within the typical range reported for P(3HB-*co*-3HHx)-based materials, supporting that SPO-derived polymerization retained the characteristic thermal behavior of 3HHx-containing PHA copolymers [25,28].

The SPO-derived film also showed clear time-dependent biodegradation (Fig. 8). For biodegradation analysis, the film was incubated in MB medium with *Microbulbifer* sp. SOL66, a marine PHA-degrading strain previously reported to exhibit strong degradation activity toward PHA materials [23]. During incubation, the residual polymer decreased progressively, while degradation increased over time. Approximately 40% degradation was observed by day 3, ~80% by day 5, and >90% by day 7, indicating near-complete degradation. These results

411 confirm that SPO-derived P(3HB-*co*-3HHx) retains high biodegradability, consistent with
412 previous reports using *Microbulbifer* sp. SOL66 [23,24].
413

414 **4. Discussion**

415 In this study, SPO was shown to be a suitable carbon source for producing P(3HB-*co*-3HHx)
416 using *C. necator* H16 harboring pCB81. Compared with other carbon sources, SPO supported
417 higher biomass formation and polymer production while enabling synthesis of a 3HHx-
418 containing copolymer, unlike fructose alone. Optimization of cultivation conditions
419 demonstrated that production could be improved through control of substrate concentration,
420 nitrogen source, fructose co-feeding, agitation speed, temperature, and emulsification. Fructose
421 co-feeding enhanced both growth and polymer accumulation, whereas Tween-based
422 emulsification improved oil utilization and copolymer production, and SDS showed inhibitory
423 effects. These findings highlight that carbon source composition, cultivation strategy, and
424 substrate accessibility are important determinants of PHA production efficiency.[6,7,26]
425 The polymer produced from SPO was successfully processed into films with defined
426 molecular, thermal, surface, and mechanical properties. The resulting P(3HB-*co*-3HHx) film
427 exhibited rapid biodegradation by *Microbulbifer* sp. SOL66, confirming its biodegradable
428 nature[17,22–24]. Although no pronounced odor or discoloration was observed, these features
429 were not quantitatively evaluated. Overall, these results demonstrate that SPO can be effectively
430 valorized as a sericulture-derived feedstock for producing value-added PHA copolymers,
431 supporting its potential for sustainable polymer production.
432

## Statements and Declarations


### Funding

This work was supported by the National Research Foundation of Korea (NRF) [RS-2022-NR070084] and the Technology Innovation Program (RS-2025-13482968, 02219753, 00467186, and 20025698) funded by the Ministry of Trade, Industry & Resources (MOTIR, Korea).


### Competing interests

The authors declare no competing financial interests or personal relationships that could have influenced the work reported in this study.

### Ethics approval

This article does not contain any studies with human participants or animal perfomed by any of the authors.

### Author contributions

**Geon Woo Doh**: Conceptualization, Visualization, Writing – original draft, Formal analysis, Data curation. **Yuni Shin**: Methodology, Formal analysis, Data curation. **Tae Yun Kim**: Methodology, Resources. **Seung Hun Lee**: Visualization, Investigation. **Yun-Gon Kim**: Validation, Formal analysis. **Hee Taek Kim**: Validation, Investigation**. Woo-Young Jeon**: Validation, Visualization**. Jungoh Ahn**: Validation, Resources. **Kwon-Young Choi**: Validation,

Data curation. **Shashi Kant Bhatia**: Data curation, visualization. **Yung-Hun Yang**: Conceptualization, supervision, writing-review and editing, project administration.

**Data availability statement:** All data related to this study are provided in the manuscript and associated files.

## References


[1] A. Beniwal, D. Mahapatara, M. Das, S. Acharjee, J. Sarma, A. Shome, A. Madhab Baruah, Vikram, A comprehensive review on the multifaceted applications of mulberry silkworm pupae: A sustainable resource, J. Asia. Pac. Entomol. 27 (2024). https://doi.org/10.1016/j.aspen.2024.102312.

[2] J. Tangsanthatkun, M. Peanparkdee, W. Katekhong, T. Harnsilawat, C.P. Tan, U. Klinkesorn, Application of Aqueous Saline Process to Extract Silkworm Pupae Oil (Bombyx mori): Process Optimization and Composition Analysis, Foods 11 (2022). https://doi.org/10.3390/foods11030291.

[3] A. Sadat, T. Biswas, M.H. Cardoso, R. Mondal, A. Ghosh, P. Dam, J. Nesa, J. Chakraborty, D. Bhattacharjya, O.L. Franco, D. Gangopadhyay, A.K. Mandal, Silkworm pupae as a future food with nutritional and medicinal benefits, Curr. Opin. Food Sci. 44 (2022). https://doi.org/10.1016/j.cofs.2022.100818.

[4] Y. Bae, J. Choi, Consumer acceptance of edible insect foods: An application of the extended theory of planned behavior, Nutr. Res. Pract. 15 (2021) 122–135. https://doi.org/10.4162/nrp.2021.15.1.122.

[5] Y. Zhou, S. Zhou, H. Duan, J. Wang, W. Yan, Silkworm Pupae: A Functional Food with Health Benefits for Humans, Foods 11 (2022). https://doi.org/10.3390/foods11111594.

[6] S. Bellini, T. Tommasi, D. Fino, Poly(3-hydroxybutyrate) biosynthesis by Cupriavidus necator: A review on waste substrates utilization for a circular economy approach, Bioresour. Technol. Rep. 17 (2022). https://doi.org/10.1016/j.biteb.2022.100985.

[7] L. Zhang, Z. Jiang, T.H. Tsui, K.C. Loh, Y. Dai, Y.W. Tong, A Review on Enhancing Cupriavidus necator Fermentation for Poly(3-hydroxybutyrate) (PHB) Production From Low-Cost Carbon Sources, Front. Bioeng. Biotechnol. 10 (2022). https://doi.org/10.3389/fbioe.2022.946085.

[8] X. Fu, H. Xu, Q. Zhang, J. Xi, H. Zhang, M. Zheng, B. Xi, L. Hou, A review on polyhydroxyalkanoates production from various organic waste streams: Feedstocks, strains, and production strategy, Resour. Conserv. Recycl. 198 (2023). https://doi.org/10.1016/j.resconrec.2023.107166.

[9] N.O. Zhila, E.G. Kiselev, V. V. Volkov, O.Y. Mezenova, K.Y. Sapozhnikova, E.I. Shishatskaya, T.G. Volova, Properties of Degradable Polyhydroxyalkanoates Synthesized from New Waste Fish Oils (WFOs), Int. J. Mol. Sci. 24 (2023). https://doi.org/10.3390/ijms241914919.

[10] K. Sangkharak, N. Paichid, T. Yunu, S. Klomklao, P. Prasertsan, Utilisation of tuna condensate waste from the canning industry as a novel substrate for polyhydroxyalkanoate production, (n.d.). https://doi.org/10.1007/s13399-019-00581-4/Published.

[11] D. V. Thuoc, V.T.M. Anh, Bioconversion of Crude Fish Oil Into Poly-3-hydroxybutyrate by Ralstonia sp. M91, Appl. Biochem. Microbiol. 57 (2021) 219–225. https://doi.org/10.1134/S0003683821020162.

[12] S.L. Riedel, S. Jahns, S. Koenig, M.C.E. Bock, C.J. Brigham, J. Bader, U. Stahl, Polyhydroxyalkanoates production with Ralstonia eutropha from low quality waste animal fats, J. Biotechnol. 214 (2015) 119–127. https://doi.org/10.1016/j.jbiotec.2015.09.002.

[13] B. Gutschmann, M. Maldonado Simões, T. Schiewe, E.S. Schröter, M. Münzberg, P. Neubauer, A. Bockisch, S.L. Riedel, Continuous feeding strategy for polyhydroxyalkanoate production from solid waste animal fat at laboratory- and pilot-scale, Microb. Biotechnol. 16 (2023) 295–306. https://doi.org/10.1111/1751-7915.14104.

[14] Y. Shin, H.J. Kim, T.R. Choi, S.J. Oh, S. Kim, Y. Lee, S. Choi, J. Oh, S.Y. Kim, Y.S. Lee, Y.H. Choi, S.K. Bhatia, Y.H. Yang, Identification of Oil-Loving Cupriavidus necator BM3-1 for Polyhydroxyalkanoate Production and Assessing Contribution of Exopolysaccharide for Vegetable Oil Utilization, Polymers (Basel). 16 (2024). https://doi.org/10.3390/polym16121639.

[15] T. Jiang, T. Tan, Z. Zong, D. Fan, J. Wang, Y. Qiu, X. Teng, H.M. Zhang, C. Rao, Enhancing oil feedstock utilization for high-yield low-carbon polyhydroxyalkanoates industrial bioproduction, Metab. Eng. 91 (2025) 44–58. https://doi.org/10.1016/j.ymben.2025.04.001.

[16] S. Obruca, I. Marova, O. Snajdar, L. Mravcova, Z. Svoboda, Production of poly(3-hydroxybutyrate-co-3-hydroxyvalerate) by Cupriavidus necator from waste rapeseed oil using propanol as a precursor of 3-hydroxyvalerate, Biotechnol. Lett. 32 (2010) 1925–1932. https://doi.org/10.1007/s10529-010-0376-8.

[17] S.J. Oh, T.R. Choi, H.J. Kim, N. Shin, J.H. Hwang, H.J. Kim, S.K. Bhatia, W. Kim, Y.J. Yeon, Y.H. Yang, Maximization of 3-hydroxyhexanoate fraction in poly(3-hydroxybutyrate-co-3-hydroxyhexanoate) using lauric acid with engineered Cupriavidus necator H16, Int. J. Biol. Macromol. 256 (2024). https://doi.org/10.1016/j.ijbiomac.2023.128376.

[18] J. Welch, J. Wallace, A.B. Lansley, C. Roper, Evaluation of the toxicity of sodium dodecyl sulphate (SDS) in the MucilAir™ human airway model in vitro, Regulatory Toxicology and Pharmacology 125 (2021). https://doi.org/10.1016/j.yrtph.2021.105022.

[19] B.A. Kerwin, Polysorbates 20 and 80 used in the formulation of protein biotherapeutics: Structure and degradation pathways, J. Pharm. Sci. 97 (2008) 2924–2935. https://doi.org/10.1002/jps.21190.

[20] N. Solak Erdem, N. Alawani, C. Wesdemiotis, Characterization of polysorbate 85, a nonionic surfactant, by liquid chromatography vs. ion mobility separation coupled with tandem mass spectrometry, Anal. Chim. Acta 808 (2014) 83–93. https://doi.org/10.1016/j.aca.2013.07.026.

[21] D.M. Ćirin, M.M. Poša, V.S. Krstonošić, M.L. Milanovič, Konduktometrijsko ispitivanje mešovitih micela na-dodecilsulfata i nejonskog surfaktanta (Triton X-100, Tween 20, Tween 60, Tween 80 ili Tween 85) u vodenim rastvorima, Hem. Ind. 66 (2012) 21–28. https://doi.org/10.2298/HEMIND110612059C.

[22] T.R. Choi, G. Lim, Y. Han, J.M. Jeon, S.K. Bhatia, H.J. Park, J.C. Joo, H.T. Kim, J.J. Yoon, Y.H. Yang, Retainment of Poly(3-hydroxybutyrate-co-3-hydroxyhexanoate) Properties from Oil-Fermented Cupriavidus necator Using Additional Ethanol-Based Defatting Process, Polymers (Basel). 17 (2025). https://doi.org/10.3390/polym17152058.

[23] S.L. Park, J.Y. Cho, S.H. Kim, S.K. Bhatia, R. Gurav, S.H. Park, K. Park, Y.H. Yang, Isolation of microbulbifer sp. Sol66 with high polyhydroxyalkanoate-degrading activity from the marine environment, Polymers (Basel). 13 (2021). https://doi.org/10.3390/polym13234257.

[24] J.Y. Cho, S.H. Kim, H.J. Jung, D.H. Cho, B.C. Kim, S.K. Bhatia, J. Ahn, J.M. Jeon, J.J. Yoon, J. Lee, Y.H. Yang, Finding a Benign Plasticizer to Enhance the Microbial Degradation of Polyhydroxybutyrate (PHB) Evaluated by PHB Degrader Microbulbifer sp. SOL66, Polymers (Basel). 14 (2022). https://doi.org/10.3390/polym14173625.

[25] N. Shin, S.H. Kim, J. Oh, S. Kim, Y. Lee, Y. Shin, S. Choi, S.K. Bhatia, J.M. Jeon, J.J. Yoon, J.C. Joo, Y.H. Yang, Evaluation of Blended Poly(3-hydroxybutyrate-co-3-hydroxyhexanoate) Properties Containing Various 3HHx Monomers, Polymers (Basel). 16 (2024). https://doi.org/10.3390/polym16213077.

[26] P. Murugan, C.Y. Gan, K. Sudesh, Biosynthesis of P(3HB-co-3HHx) with improved molecular weights from a mixture of palm olein and fructose by Cupriavidus necator Re2058/pCB113, Int. J. Biol. Macromol. 102 (2017) 1112–1119. https://doi.org/10.1016/j.ijbiomac.2017.05.006.

[27] H. Abe, Y. Doi, Side-chain effect of second monomer units on crystalline morphology, thermal properties, and enzymatic degradability for random copolyesters of (R)-3-hydroxybutyric acid with (R)-3-hydroxyalkanoic acids, Biomacromolecules 3 (2002) 133–138. https://doi.org/10.1021/bm0155975.

[28] H.J. Tang, S.Z. Neoh, K. Sudesh, A review on poly(3-hydroxybutyrate-co-3-hydroxyhexanoate) [P(3HB-co-3HHx)] and genetic modifications that affect its production, Front. Bioeng. Biotechnol. 10 (2022). https://doi.org/10.3389/fbioe.2022.1057067.

## Tables

**Table 1. Previous studies on oil-based substrates for PHA production**

| Substrate Type | Substrate | Strain | PHA Type | Yield (g/L) | Reference |
|---|---|---|---|---|---|
| Animal oil | Fish oil | *Cupriavidus necator* B-10646 | P(3HB), P(3HB-*co*-3HV-*co*-3HHx) | 3.31 | [9] |
| | Tuna condensate waste | *C. necator* TISTR 1095 | P(3HB-*co*-3HV) | 3.8 | [10] |
| | Crude fish oil | *Ralstonia* sp. isolates | P(3HB) | 0.72 | [11] |
| | | *Ralstonia* sp. M19 | | 2.7 | |
| | Animal fats | *Ralstonia eutropha* H16 | P(3HB) | 4 | [12] |
| | | Re2058/pCB113 | P(3HB-*co*-3HHx) | 3 | |
| | Waste pork fat | Re2058/pCB113 | P(3HB-*co*-3HHx) | 45.6 | [13] |
| Vegetable oil | Bean oil | *C. necator* BM3-1 | P(3HB-*co*-3HHx) | 37.1 | [14] |
| | palm oil, crude waste cooking oil | H16ΔA3043/lipAB | P(3HB-*co*-3HV) | 264 | [15] |
| | Rapeseed oil | *C. necator* H16 | P(3HB) | 105 | [16] |
| Insect oil | Pupa oil | *C. necator* H16/pCB81 | P(3HB)<br>P(3HB-*co*-3HHx) | 20 | In This study |

550 **Table 2. Silkworm Pupa oil(SPO) composition**

| Fatty acid | Abbreviation | Composition (%) |
|---|---|---|
| Hexadecanoic acid (Palmitic acid) | C16:0 | 16.8 |
| 9,12-Octadecadienoic acid (Linoleic acid) | C18:2 | 28.8 |
| 9-Octadecenoic acid (Oleic acid) | C18:1 | 53.5 |
| **Cyclopropane containing fatty acid** | | |
| Cyclopropanebutanoic acid | | 0.80 |

551

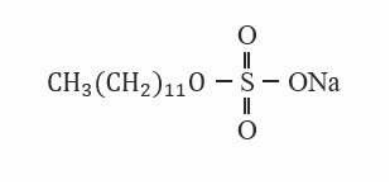
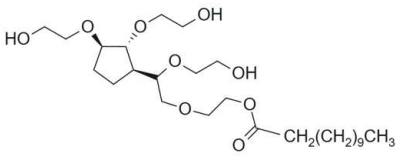
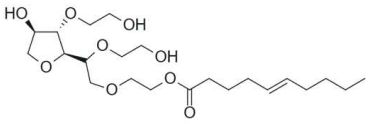
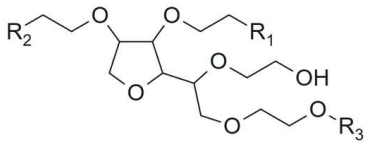
552 **Table 3. Physical properties of P(3HB-*co*-10.3%3HHx) film**

| Tensile strength (MPa) | Elongation at break (%) | Young's modulus (Mpa) | Mn ($*10^5$) | Mw ($*10^6$) | PDI |
|---|---|---|---|---|---|
| 6.0 ± 0.6 | 53.4 ± 4.6 | 127.09 ± 21.3 | 9.3 ± 0.3 | 1.30 ± 0.04 | 1.4 ± 0.01 |
| **Water contact angle (°)** | **Tg (℃)** | **Tm (℃)** | **Tc (℃)** | **Tmax (℃)** | **Residual mass (%)** |
| 81.4 ± 0.2 | -4.2 ± 1.7 | 163.9 ± 2.4 | 107.7 ± 2.6 | 283.6 | 8.3 |

553

554

555 **Table 4. Emulsifiers used, their chemical structures, and characteristics.**

| Chemical structure | Emulsifier | Characteristics | Reference |
|---|---|---|---|
|  | SDS | Strong anionic surfactant with high surface activity but potential cell toxicity | [18] |
|  | Tween 20 | Mild non-ionic surfactant widely used in biological and pharmaceutical systems | [19] |
|  | Tween 80 | Non-ionic surfactant widely used for emulsification and stabilization of hydrophobic compounds | [20] |
|  | Tween 85 | Non-ionic surfactant with relatively hydrophobic tail structure, suitable for oil-phase emulsification | [21] |

556

557

## Figure Legends

**Figure 1.** **Examination of SPO as a carbon source for PHA production.** (a) Fatty acid composition of SPO analyzed by GC–MS. (b) Comparison of PHA production using different carbon sources.

**Figure 2.** **PHB production in *Cupriavidus necator* H16 under different conditions.** (a) Effect of oil concentration. (b) Effect of nitrogen sources.

**Figure 3.** **Time-course analysis of growth and P(3HB-*co*-3HHx) accumulation in *Cupriavidus necator* H16 harboring pCB81** (a) 1% fructose as the sole carbon source. (b) 1.5% SPO as the sole carbon source. (c) Combined carbon sources (1% fructose + 1.5% SPO).

**Figure 4.** **Fructose consumption rate and PHA production under different carbon source conditions**. (a) 1% fructose as the sole carbon source. (b) 1% Fructose + 1.5% SPO. (c) Optimization of fructose concentration for PHB production with 1.5% SPO.

**Figure 5.** **Optimization of cultivation conditions for PHB production.** (a) Effect of agitation speed. (b) Effect of temperature.

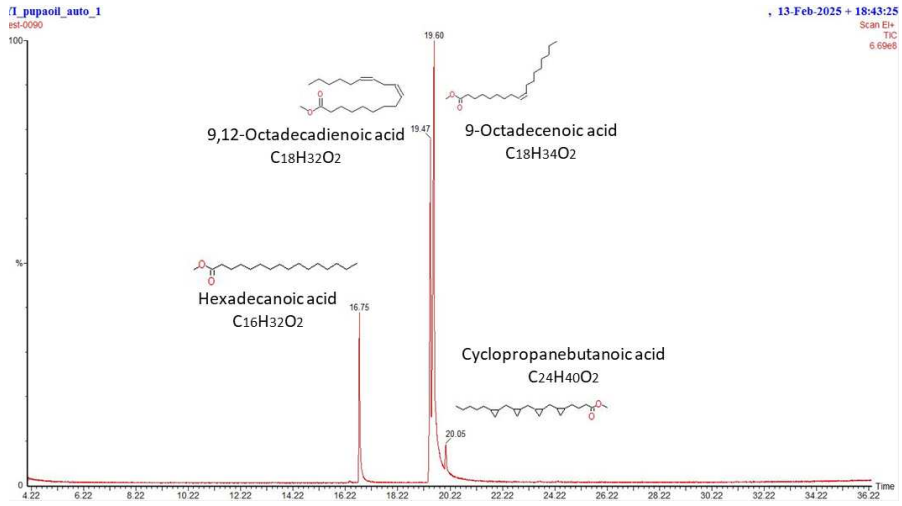
**Figure 6.** **Effect of emulsifier type and concentration on PHA production and composition.** (a) Microscopic observation of oil dispersion with and without emulsifiers. (b) Biomass growth and PHA production under different emulsifier types and concentrations.

**Figure 7.** **Time dependent monitoring of PHA production under optimized conditions.**

**Figure 8.** **Time dependent analysis of biodegradation of P(3HB-*co*-3HHx) films.**

582 **Figure 1.**

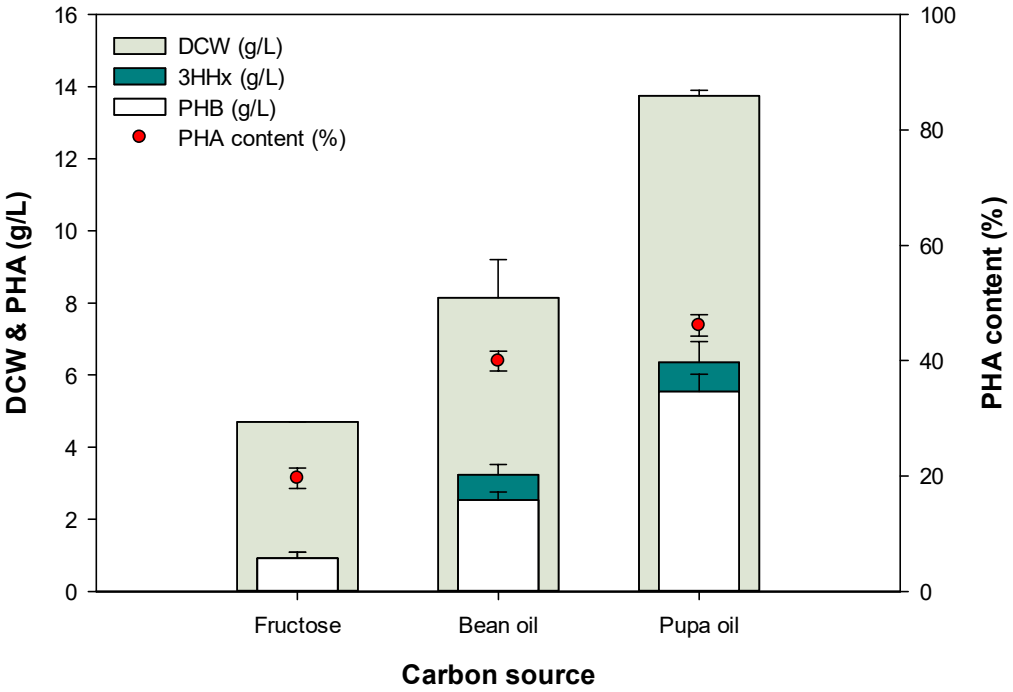
583 **(a)**




584

585

586 **(b)**

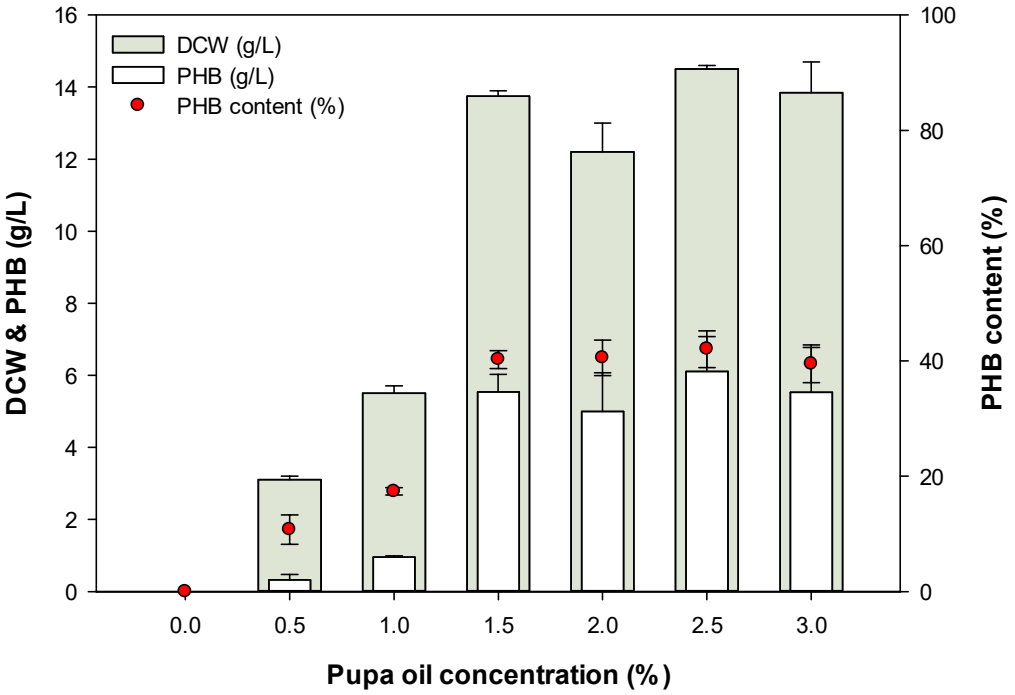



587

588

589 **Figure 2.**

590 **(a)**




591

592

593

**(b)**

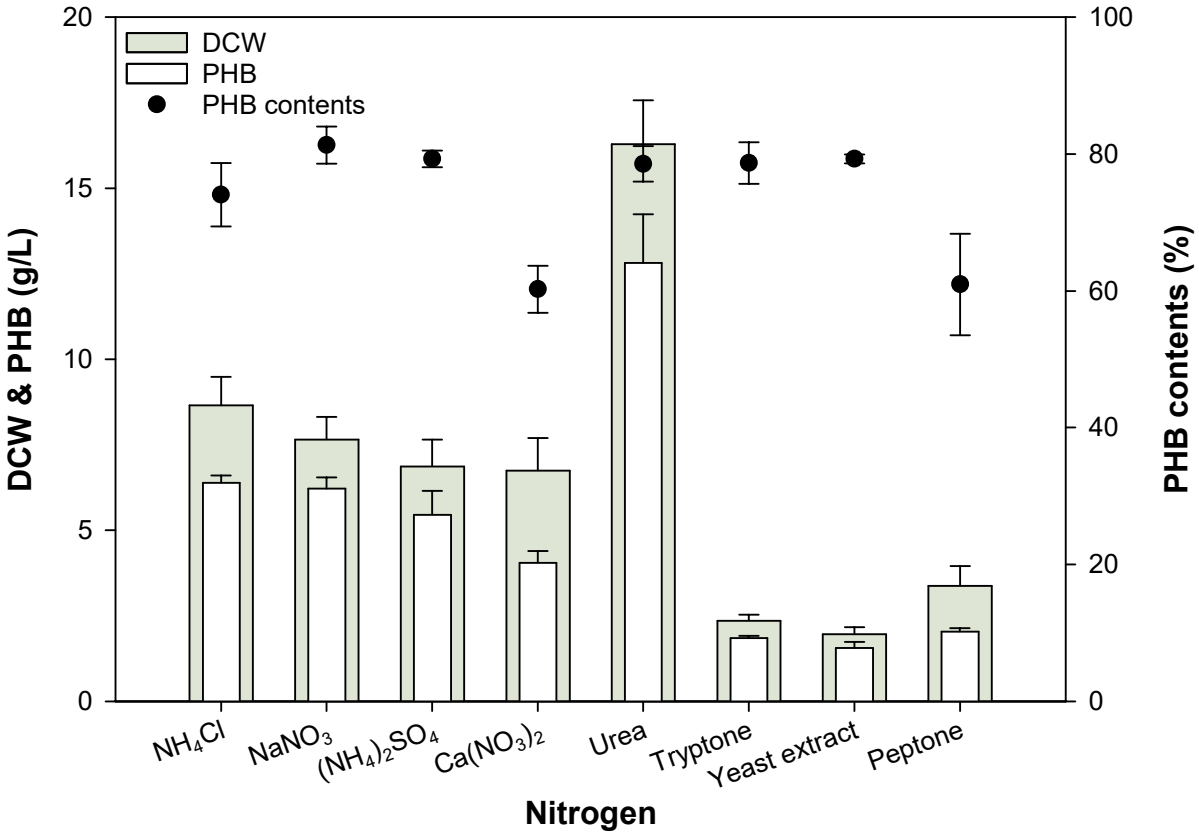
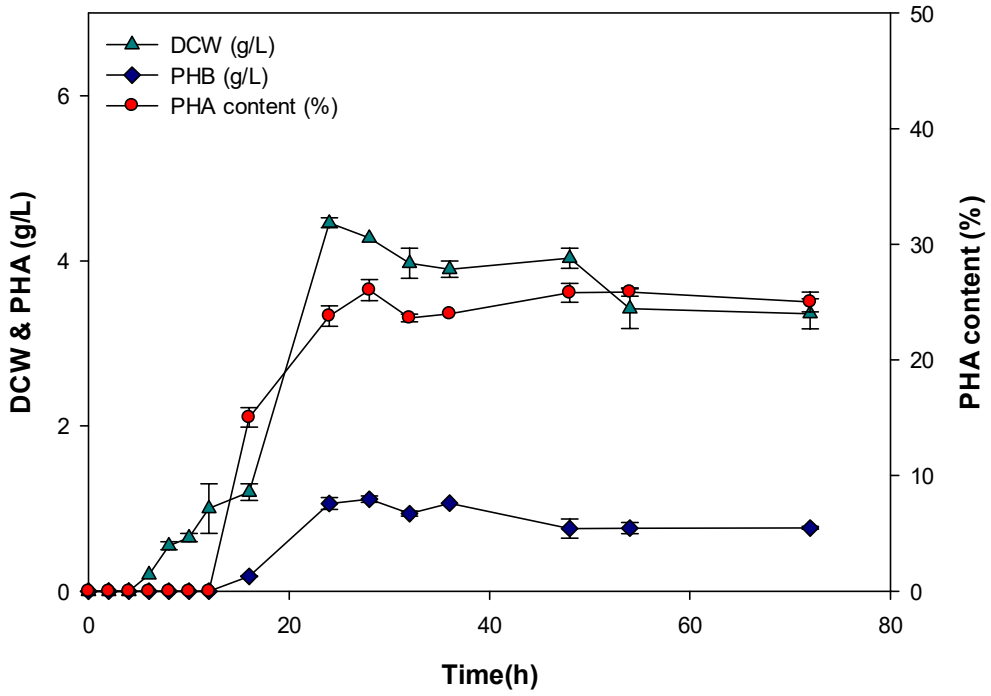
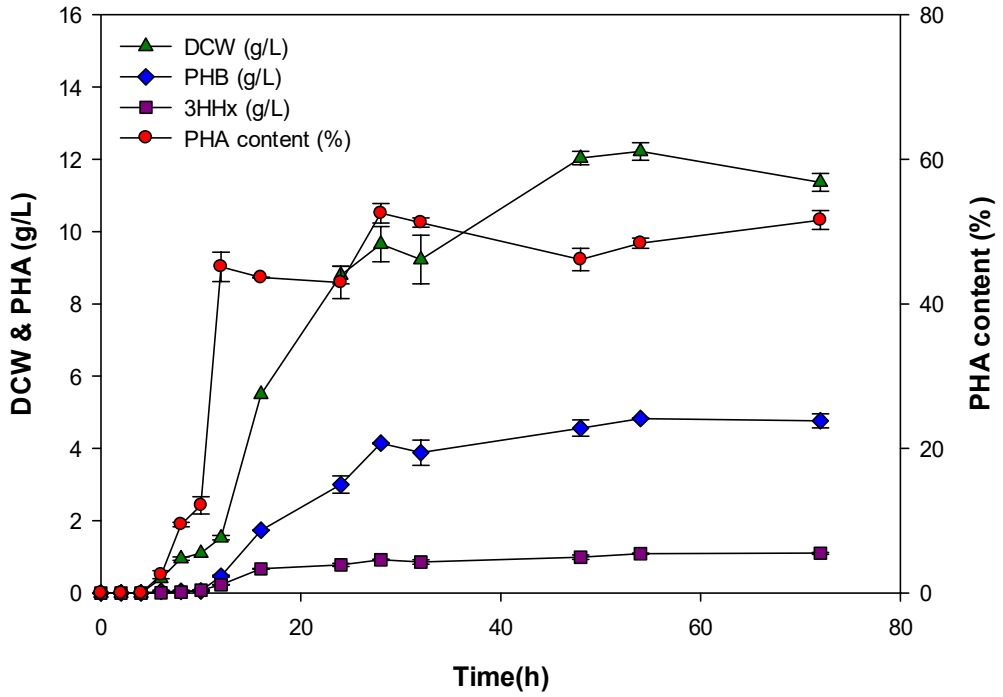

DCW
PHB
PHB contents
DCW & PHB (g/L)
PHB contents (%)
0
5
10
15
20
0
20
40
60
80
100
NH4Cl
NaNO3
(NH4)2SO4
Ca(NO3)2
Urea
Tryptone
Yeast extract
Peptone
Nitrogen

**Figure 3.**

**(a)**

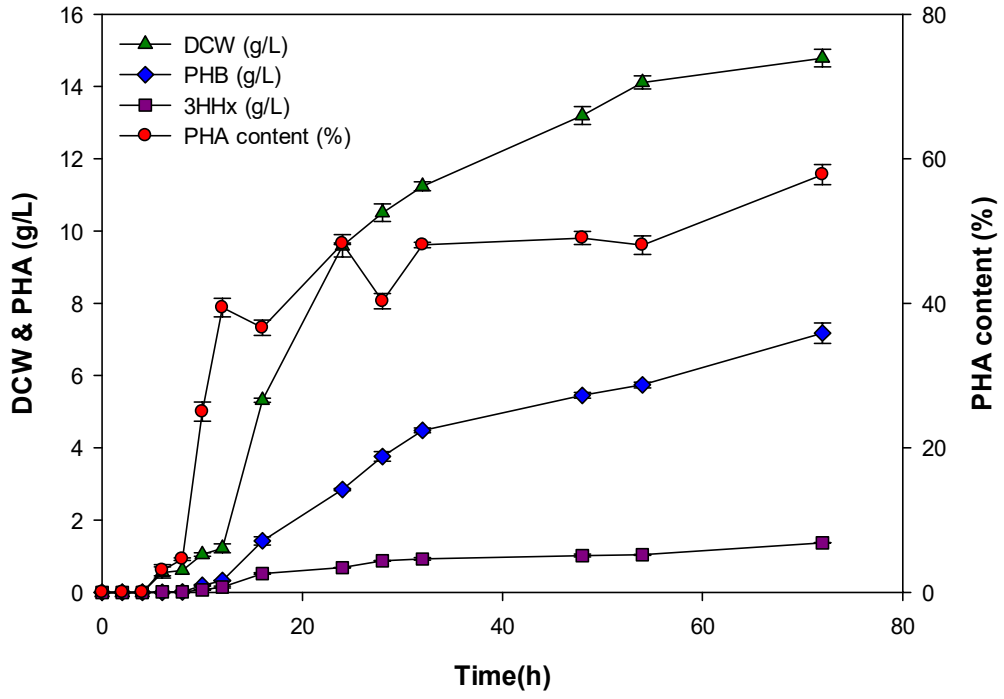

DCW (g/L)
PHB (g/L)
PHA content (%)
DCW & PHA (g/L)
PHA content (%)
Time(h)
0
2
4
6
0
10
20
30
40
50
0
20
40
60
80

**(b)**


DCW (g/L)
PHB (g/L)
3HHx (g/L)
PHA content (%)
DCW & PHA (g/L)
PHA content (%)
Time(h)
0
2
4
6
8
10
12
14
16
0
20
40
60
80
0
20
40
60
80

602

603 **(c)**

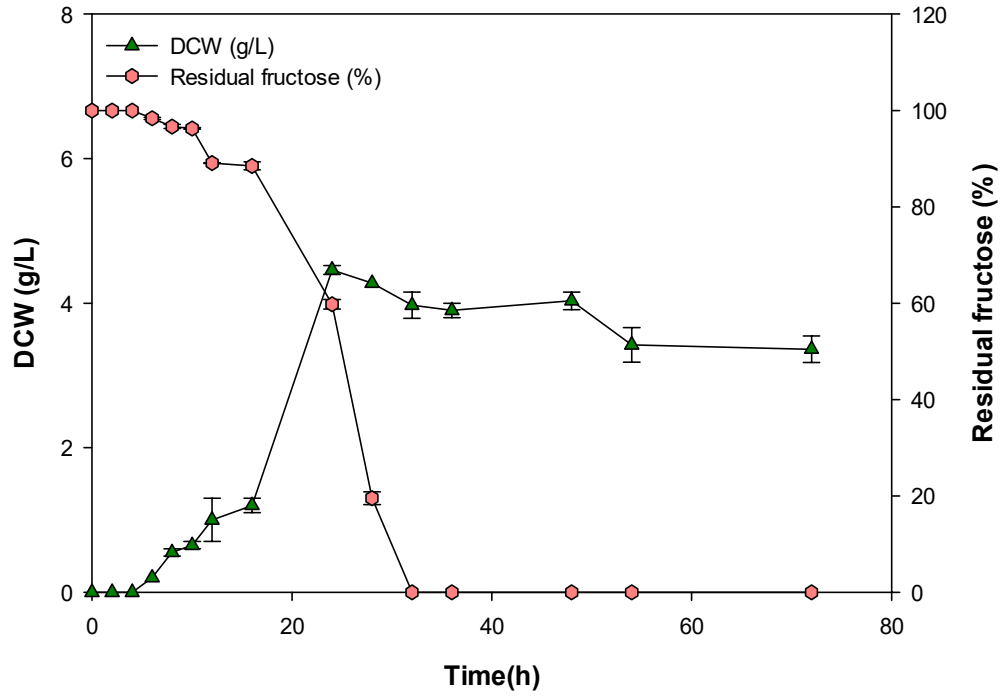

DCW (g/L)
PHB (g/L)
3HHx (g/L)
PHA content (%)
DCW & PHA (g/L)
PHA content (%)
Time(h)
0
2
4
6
8
10
12
14
16
0
20
40
60
80
0
20
40
60
80

604

605

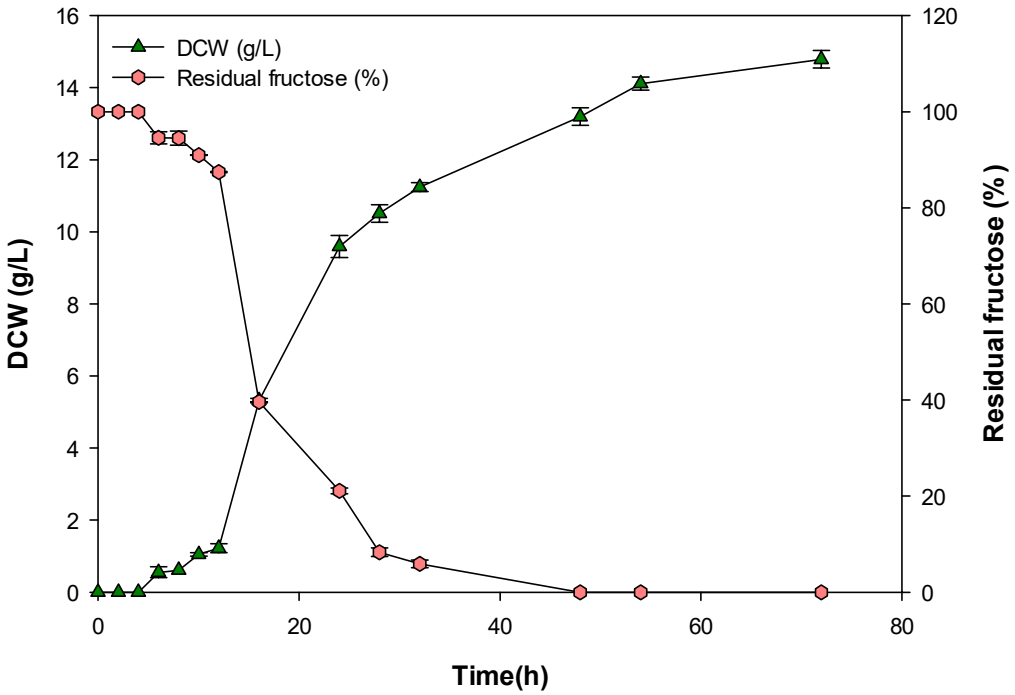
606 **Figure 4.**

607 **(a)**



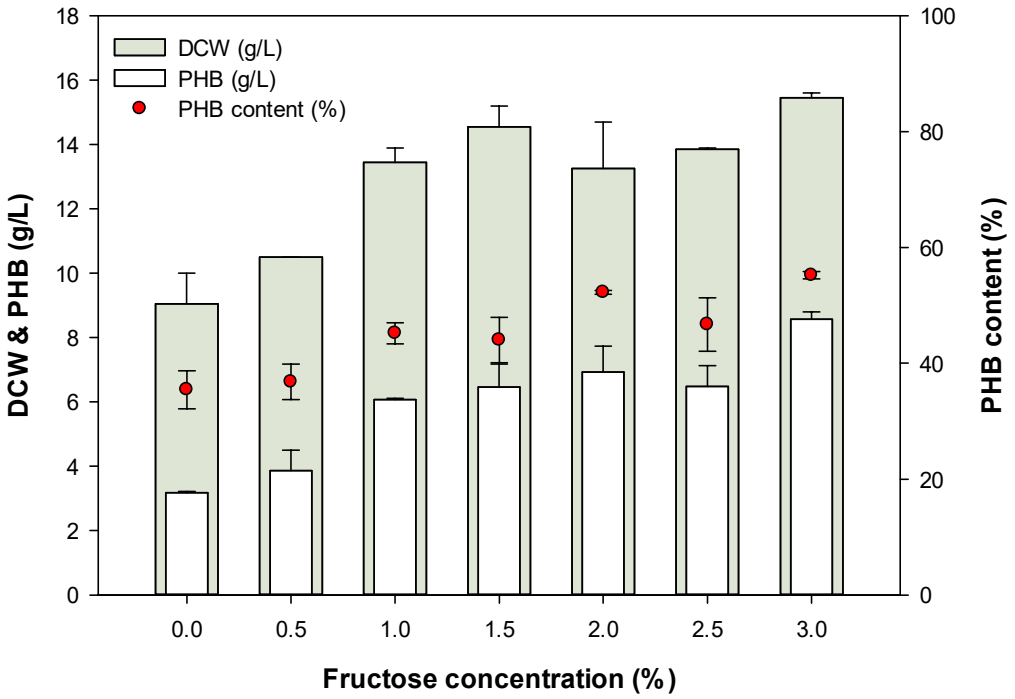

608

609 **(b)**




610

611 **(c)**

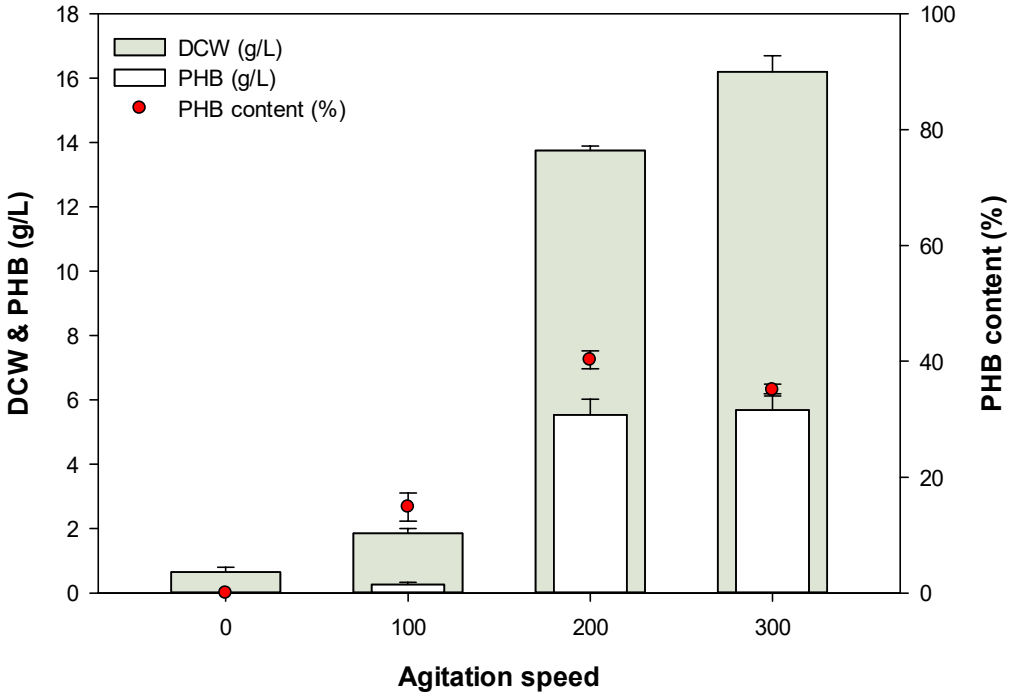

DCW (g/L)
PHB (g/L)
PHB content (%)
DCW & PHB (g/L)
PHB content (%)
Fructose concentration (%)
0.0
0.5
1.0
1.5
2.0
2.5
3.0
0
2
4
6
8
10
12
14
16
18
0
20
40
60
80
100

612

613

**Figure 5.**

**(a)**


DCW (g/L)
PHB (g/L)
PHB content (%)
DCW & PHB (g/L)
PHB content (%)
Agitation speed
0
100
200
300
0
2
4
6
8
10
12
14
16
18
0
20
40
60
80
100

**(b)**

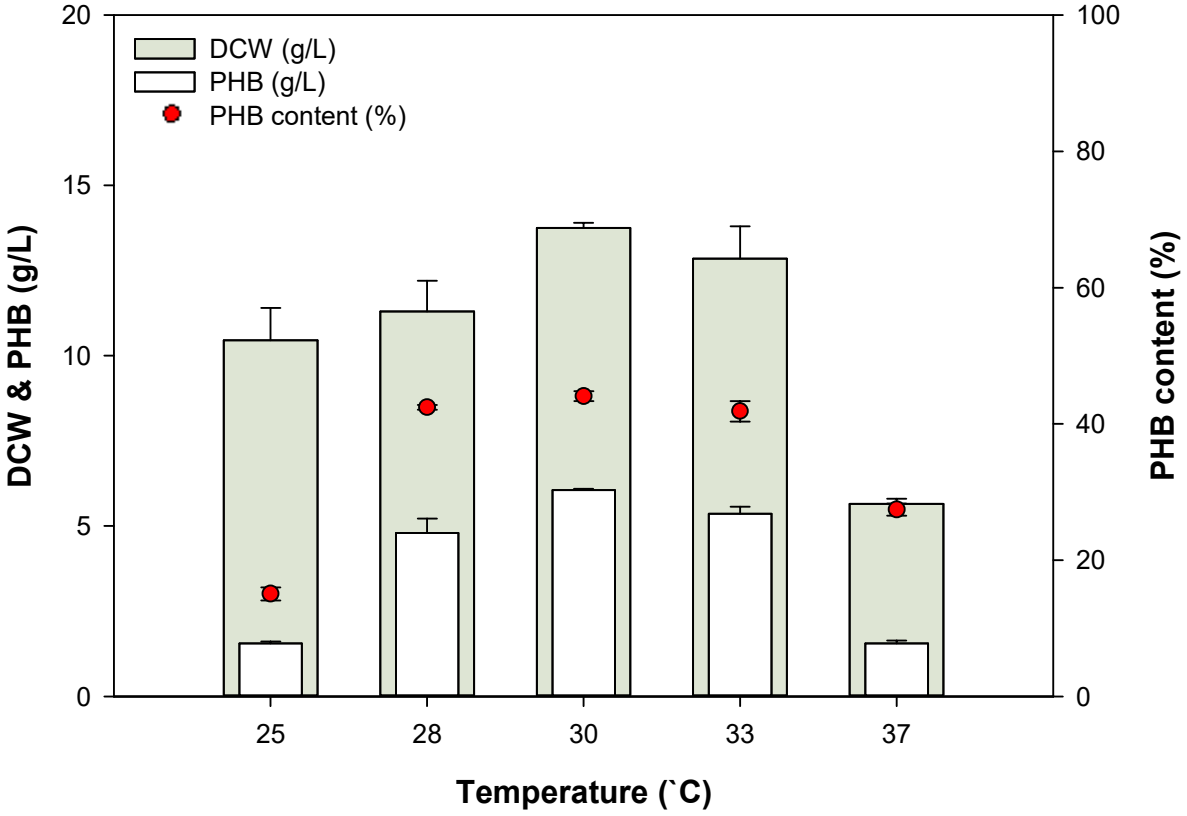
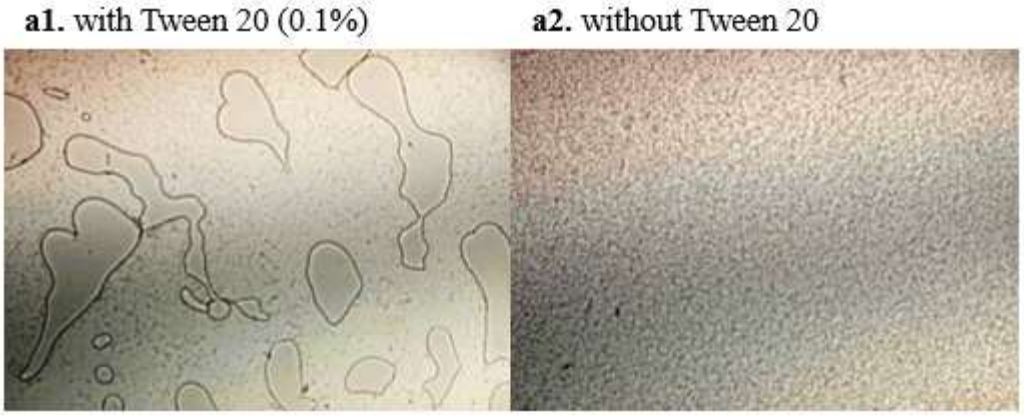
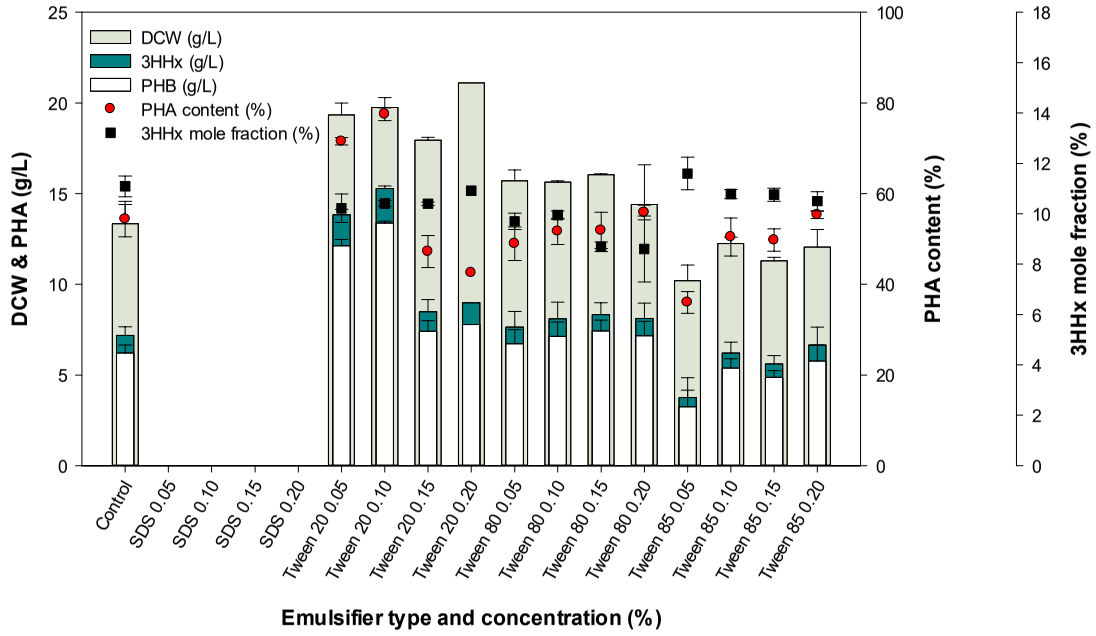

DCW (g/L)
PHB (g/L)
PHB content (%)
DCW & PHB (g/L)
PHB content (%)
Temperature (`C)
25
28
30
33
37
0
5
10
15
20
0
20
40
60
80
100

**Figure 6.**

**(a)**

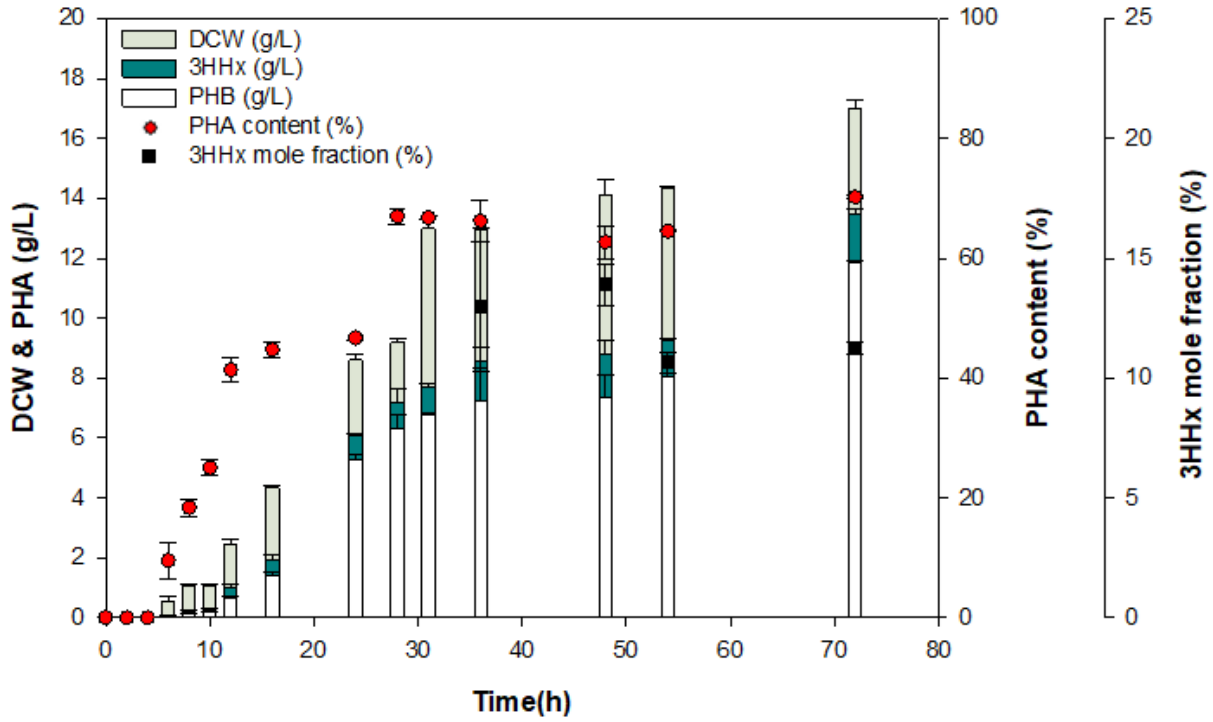

a1. with Tween 20 (0.1%)
a2. without Tween 20

**(b)**


DCW (g/L)
3HHx (g/L)
PHB (g/L)
PHA content (%)
3HHx mole fraction (%)
DCW & PHA (g/L)
PHA content (%)
3HHx mole fraction (%)
Control
SDS 0.05
SDS 0.10
SDS 0.15
SDS 0.20
Tween 20 0.05
Tween 20 0.10
Tween 20 0.15
Tween 20 0.20
Tween 80 0.05
Tween 80 0.10
Tween 80 0.15
Tween 80 0.20
Tween 85 0.05
Tween 85 0.10
Tween 85 0.15
Tween 85 0.20
Emulsifier type and concentration (%)

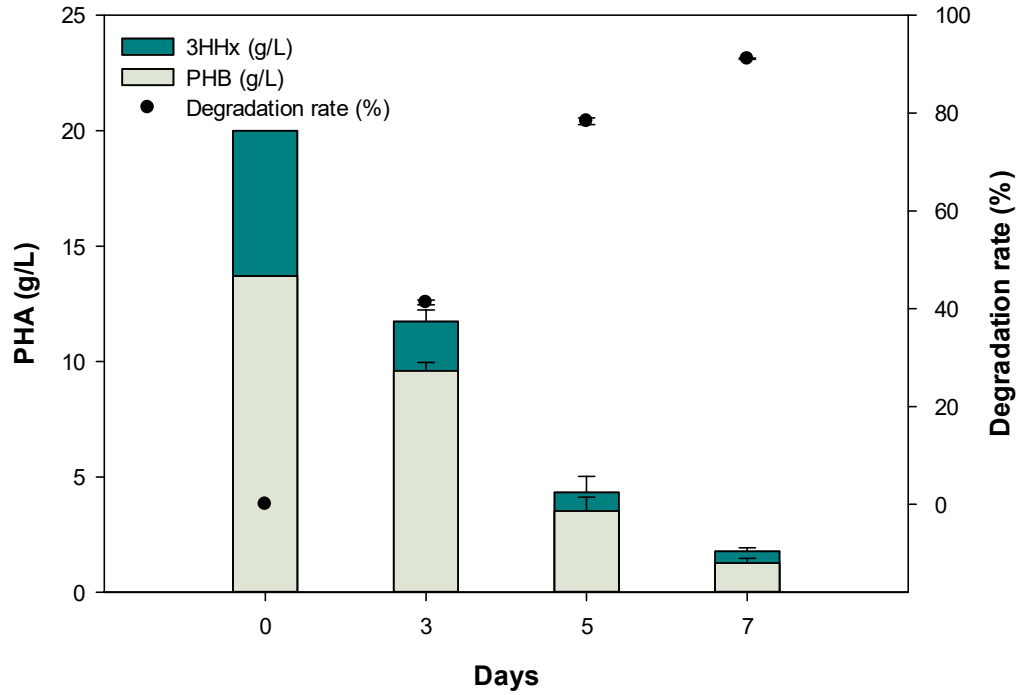
625 **Figure 7.**

626




627

628 **Figure 8.**




629

630